REVIEW OF SCIENTIFIC INSTRUMENTS **85**, 054704 (2014)

Cross-correlation measurement of quantum shot noise using homemade transimpedance amplifiers

Masayuki Hashisaka,[1,a)] Tomoaki Ota,[1] Masakazu Yamagishi,[1] Toshimasa Fujisawa,[1] and Koji Muraki[2]

[1]*Department of Physics, Tokyo Institute of Technology, 2-12-1-H81 Ookayama, Meguro, Tokyo 152-8551, Japan*
[2]*NTT Basic Research Laboratories, NTT Corporation, 3-1 Morinosato-Wakamiya, Atsugi, Kanagawa 243-0198, Japan*

(Received 8 March 2014; accepted 27 April 2014; published online 20 May 2014)

We report a cross-correlation measurement system, based on a new approach, which can be used to measure shot noise in a mesoscopic conductor at milliKelvin temperatures. In contrast to other measurement systems in which high-speed low-noise voltage amplifiers are commonly used, our system employs homemade transimpedance amplifiers (TAs). The low input impedance of the TAs significantly reduces the crosstalk caused by unavoidable parasitic capacitance between wires. The TAs are designed to have a flat gain over a frequency band from 2 kHz to 1 MHz. Low-noise performance is attained by installing the TAs at a 4 K stage of a dilution refrigerator. Our system thus fulfills the technical requirements for cross-correlation measurements: low noise floor, high frequency band, and negligible crosstalk between two signal lines. Using our system, shot noise generated at a quantum point contact embedded in a quantum Hall system is measured. The good agreement between the obtained shot-noise data and theoretical predictions demonstrates the accuracy of the measurements.
 [http://dx.doi.org/10.1063/1.4875588]

I. INTRODUCTION

Shot noise is a current fluctuation caused by the particle nature of electrons. In mesoscopic systems, where only a small number of electrons contribute to transport, shot noise provides a sensitive probe of quantum nature and many-body effects of electrons.[1] For example, in the last two decades, shot noise has been measured to demonstrate the fractional charge of quasiparticles in fractional quantum Hall (QH) systems[2,3] and spin-dependent transport in a quantum point contact (QPC).[4–6] In most of these experiments, fluctuation in one current (auto correlation $S_a = \langle \Delta I^2 \rangle$) has been measured to study shot noise, where ΔI is the deviation of current I from its time-averaged value $\langle I \rangle$. On the other hand, recent theoretical studies have indicated the immense potential of measuring cross correlation $S_X = \langle \Delta I_A \Delta I_B \rangle$ between two distinct currents (I_A and I_B); the effect of quantum statistics and two-particle interference in mesoscopic conductors can be investigated by measuring S_X.[7] However, despite their high potential, cross-correlation measurements have been performed in only a few experiments[8–12] because of the technical difficulty.

The technical requirements for cross-correlation measurements can be summarized as follows. (1) *Low noise floor*: The measurement system must have a sufficiently low noise floor to detect extremely small shot noise in mesoscopic conductors (typically below 10^{-28} A^2/Hz).[12–15] (2) *Frequency band*: In electronic devices, extrinsic $1/f$ noise and random telegraph noise mask shot noise at low frequencies.[16] Shot noise must therefore be measured in a frequency band typically above a few tens of kHz. (3) *Negligible crosstalk*: Unlike in optics, unwanted crosstalk often disturbs electronic transport measurements. In usual measurement setups for mesoscopic devices, unavoidable parasitic capacitance C_p above a few pF exists between wires. In some cases, this causes serious crosstalk in ac transport measurements, although it does not cause problems in general dc measurements. Therefore, to measure cross correlation between extremely small current fluctuations at frequencies above a few tens of kHz, it is essential to eliminate such crosstalk.

To attain low noise floor and a high-frequency band, previous experiments have employed high-speed voltage amplifiers (VAs) in both auto-[2–6,13–15] and cross-correlation[9–11] measurements. However, the high input impedance of VAs often gives rise to extrinsic noise due to crosstalk, which can be detrimental in particular to cross-correlation measurements. To overcome this technical problem, we developed a cross-correlation measurement system using homemade transimpedance amplifiers (TAs). Low noise floor was obtained by cooling the TAs to 4 K. The TAs were designed to have flat gain response up to about 1 MHz. The low input impedance Z_{in} of the TAs ($Z_{in} \ll 1/\omega C_p$) strongly reduces the crosstalk due to C_p.

To determine the performance of the developed system, we measured shot noise generated at a QPC embedded in a QH system. In cross-correlation shot-noise measurements, the Pauli exclusion principle for electrons is manifested as a negative sign for S_X.[1,8,9] The obtained data agreed well with theory[1] and the results of previous experiments,[8,9] thus showing the Fermionic nature of electrons. Electron temperature in the device was evaluated by fitting the shot-noise data to the theoretical formula.[17] These results confirm the accuracy of our measurement.

a)E-mail: hashisaka@phys.titech.ac.jp. Telephone: +81-3-5734-2809.

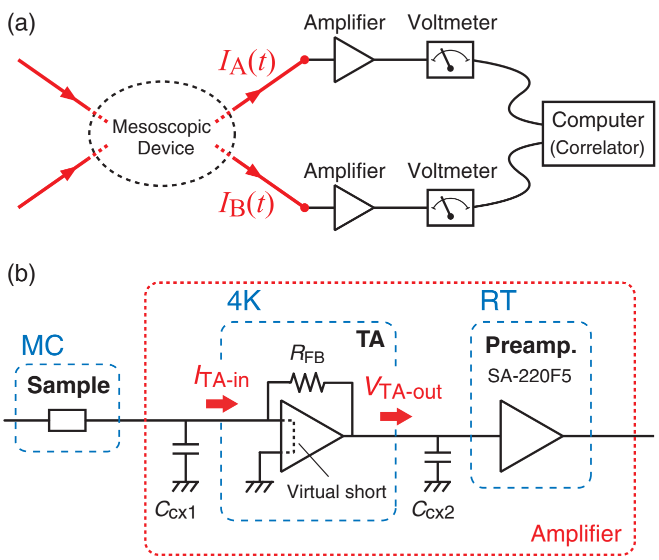

FIG. 1. (a) Overview of cross-correlation measurement system for two currents $I_A(t)$ and $I_B(t)$. (b) Schematic of amplifying system in the measurement setup.

The rest of this paper is organized as follows. In Sec. II, we give an overview of cross-correlation shot-noise measurements and compare them with auto-correlation measurements. We discuss the advantages and difficulties of measurements using TAs in comparison to conventional systems using VAs. In Sec. III, we show the performance of our homemade TA. In Sec. IV, we present shot-noise measurements and examine the effectiveness of the developed system. Section V is devoted to a summary of this study.

II. CROSS-CORRELATION MEASUREMENT USING TRANSIMPEDANCE AMPLIFIERS

A. Overview of the system

The overview of our cross-correlation measurement setup is shown in Fig. 1(a). Our measurement is aimed to evaluate the cross correlation S_X of two distinct currents $I_A(t)$ and $I_B(t)$ flowing through a mesoscopic conductor. $I_A(t)$ and $I_B(t)$ are individually amplified by two TAs. The amplified signals are recorded using a two-channel digitizer (National Instruments PXI-5922), which provides two isolated voltmeters. The original current signals are calculated from the measured voltages $V_A(t)$ and $V_B(t)$ according to $I_{A(B)}(t) = V_{A(B)}(t)/Z_{total}$, where Z_{total} is the transimpedance of the amplifier. Each channel of the digitizer retrieves 20 000 data points for a single time-domain measurement at a sampling rate of 2 MS/s. We convert $I_A(t)$ and $I_B(t)$ to current spectra $\tilde{I}_A(f)$ and $\tilde{I}_B(f)$ using the fast Fourier transform technique and then compute the cross spectral density $S_X(f)$.[1] The above procedure was repeated to acquire multiple spectral densities, which were then averaged to eliminate uncorrelated fluctuations. Finally, the cross correlation S_X was determined as the mean value of the averaged spectral density $S_X(f)$ in the frequency range from 200 to 500 kHz.

Figure 1(b) shows a schematic of the amplifying system. We prepared a pair of these setups as shown in Fig. 1(a). The sample is placed in the mixing chamber (MC), and the TAs are installed at the 4 K stage of a dilution refrigerator (Oxford Instruments Triton400). Currents from the sample flow to the TAs through 50 Ω coaxial cables with capacitance $C_{cx1} \cong 10$ pF. Each TA converts its input current $I_{TA\text{-in}}$ to voltage output as $V_{TA\text{-out}} = R_{FB} I_{TA\text{-in}}$, where R_{FB} is the negative feedback resistance. The outputs travel through 50 Ω coaxial cables with $C_{cx2} \cong 100$ pF to commercial preamplifiers (NF Corporation SA-220F5: gain 46 dB and input impedance 1 MΩ), which are at room temperature (RT). Total transimpedance is given by $Z_{total} = R_{FB} G_{pre}$, where G_{pre} is the gain of the preamplifiers.

B. Cross-correlation measurement of shot noise

Figure 2(a) shows a schematic of our shot-noise measurement using the cross-correlation technique. A current I is injected to the sample from the left Ohmic contact by applying a voltage V. I is partitioned by the QPC acting as a beam splitter (BS) to generate shot noise ($\Delta I_S = \Delta I_{S\text{-A}}$ or $\Delta I_{S\text{-B}}$) in the transmitted (I_A) and reflected (I_B) currents, which are collected at the Ohmic contacts Ω_A and Ω_B, respectively. Since each electron is either forward scattered or backscattered at the QPC, $\Delta I_{S\text{-A}}$ and $\Delta I_{S\text{-B}}$ are negatively correlated with each other as $\Delta I_{S\text{-A}} = -\Delta I_{S\text{-B}}$. We measure the current fluctuations ΔI_A and ΔI_B to obtain $S_X = \langle \Delta I_A \Delta I_B \rangle$. In this system, ΔI (ΔI_A or ΔI_B) consist of not only ΔI_S but also Johnson−Nyquist noise (ΔI_{JN}; $\Delta I_{JN\text{-A}}$ or $\Delta I_{JN\text{-B}}$) and the extrinsic noise (ΔI_{TA}; $\Delta I_{TA\text{-A}}$ or $\Delta I_{TA\text{-B}}$) generated in the amplifiers. Our purpose is to extract the shot noise from the obtained S_X.

Let us consider how to evaluate the shot noise from measured S_X rather than from auto-correlation measurements. Suppose that the total current fluctuation is given by $\Delta I = \Delta I_S + \Delta I_{JN} + \Delta I_{TA}$. Its auto correlation is calculated as $S_a = \langle \Delta I^2 \rangle = \langle \Delta I_S{}^2 \rangle + \langle \Delta I_{JN}{}^2 \rangle + \langle \Delta I_{TA}{}^2 \rangle$. Here we assume that ΔI_S, ΔI_{JN}, and ΔI_{TA} are uncorrelated with one another. In realistic experiments at a finite temperature, $\langle \Delta I_{JN}{}^2 \rangle$ and $\langle \Delta I_{TA}{}^2 \rangle$ always appear in measured S_a. On the other hand,

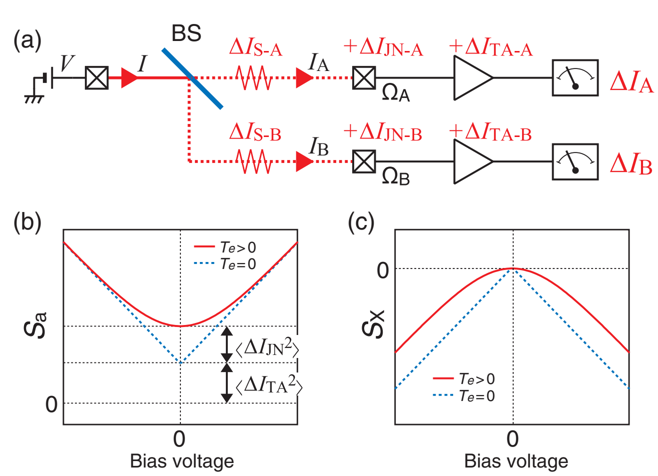

FIG. 2. (a) Schematic of shot-noise measurement. Schematic of (b) auto- and (c) cross-correlation data at finite (red solid) and zero (blue dotted lines) temperatures as a function of applied bias voltage.

in cross-correlation measurements, the shot-noise term $S_X{}^{shot} = \langle \Delta I_{S\text{-}A} \Delta I_{S\text{-}B} \rangle$ can be directly measured as $S_X = S_X{}^{shot}$. When the two amplifiers are isolated and $G_{AB} = G_{BA} = 0$, as in the case discussed in Sec. IV, fluctuations in one output terminal of the BS cannot be fed into the other terminal. Here, G_{AB} (G_{BA}) is the conductance from Ω_B (Ω_A) to Ω_A (Ω_B). Therefore, only the correlation $\Delta I_{S\text{-}A} = -\Delta I_{S\text{-}B}$ caused at the BS is measured in S_X with no contributions from ΔI_{JN} and ΔI_{TA}. Note that vanishing of the Johnson−Nyquist noise term $\langle \Delta I_{JN\text{-}A} \Delta I_{JN\text{-}B} \rangle$ at $G_{AB} = G_{BA} = 0$ is consistent with the theoretical expression $\langle \Delta I_{JN\text{-}A} \Delta I_{JN\text{-}B} \rangle = -2k_B T_e (G_{AB} + G_{BA})$,[1] where k_B is the Boltzmann constant, and T_e is electron temperature.

Theoretically, $S_X{}^{shot}$ at finite temperatures is given by

$$S_X^{shot} = -2eIF\left[\coth\left(\frac{eV}{2k_B T_e}\right) - \frac{2k_B T_e}{eV}\right], \quad (1)$$

where $F = [\Sigma_n T_n(1 - T_n)]/N$ is the shot-noise reduction factor due to the anti-bunching of electrons.[1] Here T_n is the transmission probability of the BS, where n denotes the channel label, and N is the number of channels. The negative sign of $S_X{}^{shot}$ reflects the binominal distribution of electrons and the resultant negative correlation.

The expected behaviors of auto and cross correlation as a function of bias voltage are illustrated in Figs. 2(b) and 2(c), respectively. The solid (dotted) lines represent the behavior at $T_e > 0$ ($T_e = 0$). While both ΔI_{TA} and ΔI_{JN} contribute to S_a, they do not appear in S_X when $G_{AB} = G_{BA} = 0$. This allows us to evaluate $S_X{}^{shot}$ without subtracting these components from the measured S_X. This is a great advantage of the cross-correlation technique, particularly when the extrinsic noise ΔI_{TA} is greater than the target signal ΔI_S. Whereas the noise floor is determined by $\langle \Delta I_{TA}{}^2 \rangle$ in auto-correlation measurements, the extrinsic noise term vanishes in cross-correlation measurements. Therefore, noise floor in a cross-correlation measurement can in principle be lower than that in an auto-correlation measurement.

In previously reported auto-correlation measurements, the Johnson−Nyquist noise term $\langle \Delta I_{JN}{}^2 \rangle$ at zero bias (and its dependence on the bath temperature) has been used to evaluate T_e.[18] Such a method cannot be used for cross-correlation measurements, since the $\langle \Delta I_{JN\text{-}A} \Delta I_{JN\text{-}B} \rangle$ term vanishes in the setup shown in Fig. 2(c). Nevertheless, as described by Eq. (1), the Fermi distribution at finite temperature manifests itself in the bias-voltage dependence of S_X, which allows us to evaluate T_e by fitting S_X with Eq. (1).[17] In Sec. IV C, we evaluate T_e by this method and demonstrate the performance of our measurement system.

C. Comparison of transimpedance amplifiers and voltage amplifiers

Here we compare our measurement system with conventional cross-correlation measurement setups using VAs. The effective circuit diagram of a voltage-amplifying system with a noise source is shown in Fig. 3(a). A target current fluctuation $\Delta I'$ is converted to a voltage fluctuation $\Delta V'$ by effective shunt impedance Z_{eff}, as $\Delta V' = Z_{eff} \Delta I'$, and then $\Delta V'$ is amplified by a VA of gain G. The transimpedance Z_{trans} of this system is given by $Z_{trans} = Z_{eff} G$. Generally, Z_{eff} consists of the input impedance Z_{in} of the amplifier and the impedance Z_{sam} of the sample, but additional shunt impedance Z_{add} can also be inserted deliberately. For example, inductor-capacitor (LC) circuits were inserted as Z_{add} to achieve high Z_{eff} at MHz frequencies.[12] Since Z_{in} is usually much larger than the other two impedances, Z_{eff} is given by $(Z_{eff})^{-1} \cong (Z_{add})^{-1} + (Z_{sam})^{-1}$.

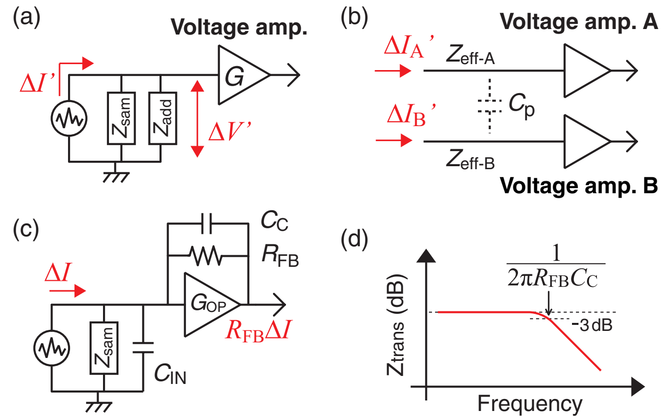

FIG. 3. (a) Effective circuit diagram of noise measurement system using a VA. (b) Schematic of cross-correlation measurement using the circuit in (a). (c) Effective circuit diagram of noise measurement system using a TA with C_{IN} at the input. (d) Bode plot of Z_{trans} of the TA in (c).

Figure 3(b) shows a schematic of a cross-correlation measurement setup using VAs. Fluctuations $\Delta I_A'$ and $\Delta I_B'$ are converted to $\Delta V_A'$ and $\Delta V_B'$ using $Z_{eff\text{-}A}$ and $Z_{eff\text{-}B}$, respectively, and are then amplified by the VAs. In this setup, it is necessary to pay attention to the following two points. First, a higher $Z_{eff\text{-}A}$ or $Z_{eff\text{-}B}$ can lead to higher crosstalk through C_p between the two signal lines. On the other hand, higher $Z_{eff\text{-}A}$ and $Z_{eff\text{-}B}$ are favorable in terms of signal amplitude, because $\Delta V_{A(B)}' = Z_{eff\text{-}A(B)} \Delta I_{A(B)}'$. Thus, when choosing shunt impedance, high sensitivity and low crosstalk are mutually exclusive. For low crosstalk and high amplitude, C_p must be below 1 pF, which is technically difficult. Second, $Z_{eff\text{-}A}$ and $Z_{eff\text{-}B}$ individually depend on the sample impedances Z_{sam1} and Z_{sam2} connected to the two signal lines, respectively. When Z_{sam1} and Z_{sam2} vary depending on the measurement parameters (e.g., temperature), not only $\Delta I_A'$ and $\Delta I_B'$ but also Z_{trans} of the measurement systems vary. This makes data analysis rather cumbersome, because to evaluate the cross correlation $\langle \Delta I_A' \Delta I_B' \rangle$, we need to evaluate the dependence of the system's performance on the measurement parameters.

In our measurement setup [Fig. 3(c)], TAs directly convert current fluctuations into voltage fluctuations as $\Delta V = R_{FB} \Delta I$. Their input impedance is given by $Z_{in} = R_{FB}/G_{OP}$, where G_{OP} is open-loop gain of the amplifier installed in the TAs. Therefore, by choosing R_{FB} value, Z_{in} can be set much lower than the typical Z_{sam} ($h/e^2 \cong 26$ kΩ) and $(\omega C_p)^{-1}$ at 1 MHz ($\cong$100 kΩ for $C_p \cong 1$ pF). This resolves the above issues as follows. First, when $Z_{in} \ll 1/\omega C_p$, the currents are fed into the TAs without interfering with each other. This leads to the two TAs being isolated. Second, because $Z_{in} \ll Z_{sam}$, $(Z_{in})^{-1} + (Z_{sam})^{-1} \cong (Z_{in})^{-1}$ holds so that the system performance is no longer affected by the variation of Z_{sam}.

While the frequency band of voltage-amplifying systems can be designed with Z_{eff} by inserting an arbitrary Z_{add}, TAs have unique frequency-response characteristics, as shown in Fig. 3(d). The upper cutoff frequency (−3dB) of a TA is given by $f_{-3dB} = (2\pi R_{FB} C_C)^{-1}$, where C_C is a phase-compensation capacitor placed in parallel with R_{FB}. Therefore, for high-frequency response, lower C_C is desirable. However, to prevent unwanted oscillation due to the phase shift induced by C_{IN} at the input of the TAs, rather large C_C has to be installed depending on the value of C_{IN}. Since higher C_C is necessary to compensate the effect of higher C_{IN}, we need to reduce C_{IN} to use smaller C_C.

III. HOMEMADE TRANSIMPEDANCE AMPLIFIER

In principle, the extrinsic noise term $\langle \Delta I_{TA\text{-}A} \Delta I_{TA\text{-}B} \rangle$ can be eliminated by time averaging in cross-correlation measurements. However, it would take a very long time to attain the required low noise floor if $\Delta I_{TA\text{-}A}$ and $\Delta I_{TA\text{-}B}$ are much larger than the shot noise. Unfortunately, input-referred noise of commercial TAs is typically above 1×10^{-24} A^2/Hz at MHz frequencies, which is not sufficiently low to measure shot noise. In addition, as discussed in Subsection II C, it is important to reduce C_{IN} to achieve a high-frequency response. In low-temperature shot-noise measurement setups, C_{IN} is dominated by the capacitance of coaxial cables [C_{CX1} in Fig. 1(b)]. To reduce the length of the coaxial cables and hence C_{IN}, TAs should be placed near the sample. For these reasons, we developed homemade TAs, which have a sufficiently low noise floor and can be operated in a refrigerator (at the 4 K stage).

Figure 4(a) shows the circuit diagram of the TAs used in this study. The TAs were made using four commercial high-electron-mobility transistors (HEMTs: Avago Technologies ATF-35143). The circuit consists of three sections: an amplifying part comprising three common-source HEMTs (H1, H2, and H3), a source-follower circuit (H4), and a negative-feedback part (R_{FB} = 33 kΩ). Each of the three common-source circuits has a gain of $G \cong -7$; hence, G_{OP} of the entire system is $G_{OP} \cong (-7)^3 \cong -350$. $Z_{in} \cong R_{FB}/G_{OP} \cong 100$ Ω is much lower than the typical sample impedance $h/e^2 \cong 26$ kΩ. The source-follower circuit sets the output impedance Z_{out} to be low (500 Ω). The 1 pF placed in parallel with R_{FB} is the phase-compensation capacitor C_C.

We fabricated two TAs of identical design and evaluated their low-temperature performance by installing them at the 4 K stage of a dilution refrigerator. For each TA, an ac voltage of 1 mV rms was applied to a 12.9 kΩ test resistor placed at the MC (MC temperature $T_{MC} \cong 15$ mK), and the output current 7.75 nA = 1 mV/12.9 kΩ was converted by the TA to a voltage signal and recorded by a digitizer. The obtained absolute transimpedance and phase of the TAs are shown in Figs. 4(b) and 4(c), respectively. Nearly the same response for each was obtained by appropriately tuning the drain and gate voltages for each TA (V_D = 2.0 V and V_G = −0.3000 V for TA1 and V_D = 2.0 V and V_G = −0.3075 V for TA2). From 2 kHz to 1 MHz, the transimpedances were constant within

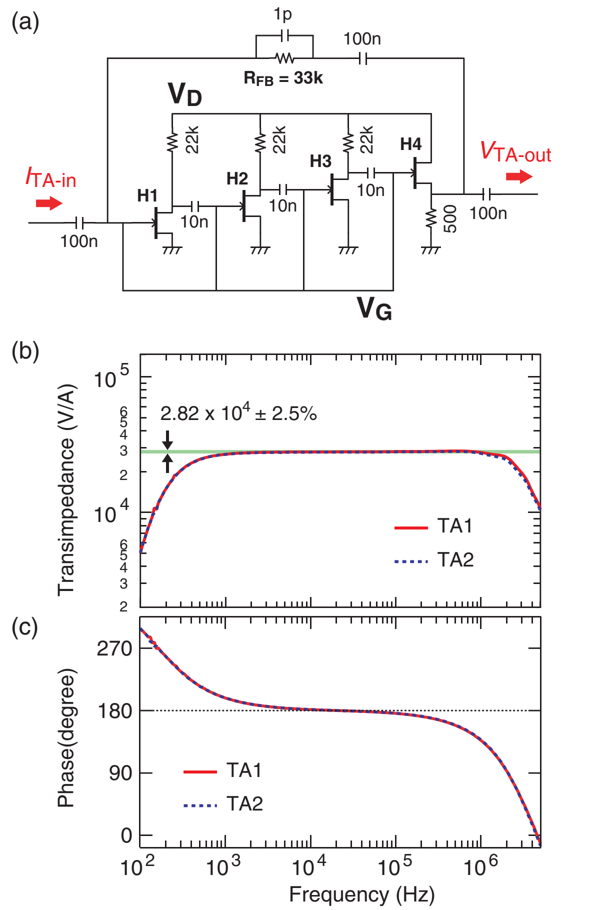

FIG. 4. (a) Circuit diagram of homemade TA. Characters H1–H4 denote ATF-35143 HEMTs. (b) Absolute transimpedance and (c) phase of TAs at 4 K measured as a function of frequency.

±2.5% of 2.82×10^4 V/A. This flat gain response over a wide frequency range is suitable for measuring white shot noise. In this frequency range, the phase stayed at about 180°, which ensures the negative feedback of the circuit. The typical energy consumption of these TAs was about 1.5 mW, which is sufficiently small for operation at 4 K. They had input-referred noise of 1×10^{-25} A^2/Hz in the frequency band of 100−600 kHz, which is one order of magnitude smaller than that of typical commercial TAs.

Let us compare the anticipated crosstalk in a cross-correlation measurement using the TAs with that of a conventional voltage-amplifying system. First, we consider a current fluctuation $\Delta I = \Delta I_{corr} + \Delta I_{non\text{-}corr}$ generated in one of the signal lines in the system shown in Fig. 3(b). Here, ΔI_{corr} is the target correlating fluctuation and $\Delta I_{non\text{-}corr}$ is the extrinsic non-correlating noise. Assuming $Z_{eff} \cong 10$ kΩ and $C_p \cong 1$ pF [$(\omega C_p)^{-1} \cong 300$ kΩ at 500 kHz], 3%−4% of ΔI flow to the other signal line. This causes serious crosstalk particularly when the system has large $\Delta I_{non\text{-}corr}$. On the other hand, when the VAs are replaced with the TAs, only 0.03%−0.04% of ΔI flow through C_p because of the small Z_{in} (≅100 Ω) of the TAs. Thus, the TAs can significantly suppress the crosstalk and improve the accuracy of cross-correlation measurements. In Sec. IV, we show that crosstalk in shot-noise measurements using the TAs is actually negligible.

IV. SHOT-NOISE MEASUREMENT

In this section, we present shot-noise measurements using the cross-correlation technique. The measurements were performed on a QH device, where currents flow along one-dimensional edge channels at the boundary of the QH region. We measured the shot noise generated at a QPC embedded in the QH system. The accuracy of our measurement is examined by comparing the data with shot-noise theory.

A. Measurement setup

Figure 5(a) shows a schematic of the device and the measurement setup. The QPC was formed in a two-dimensional electron gas (2DEG) in a $GaAs/Al_{0.3}Ga_{0.7}As$ heterostructure. The 2DEG has an electron density of $n_e = 2.3 \times 10^{11}$ cm^{-2} and a mobility of $\mu = 3.3 \times 10^6$ cm^2/Vs. The device has five Ohmic contacts (Ω_n: $n = 1-5$) and a split-gate electrode to form a QPC. The measurements were performed at $T_{\rm MC} = 15$ mK in a dilution refrigerator. An integer QH state with a bulk filling factor $\nu = 2$ was established by applying a magnetic field of 4.4 T perpendicular to the 2DEG. The field direction was such that the chirality of the edge channels was clockwise, as shown by the arrows in Fig. 5(a).

A bias voltage V_1 was applied to inject a dc current I_1 into the 2DEG from Ω_1. I_1 flowed along the edge channel and was partitioned at the QPC to generate shot noise. At Ω_3 and Ω_5, only the fluctuations in the currents passing through the coupling capacitors (100 nF) were fed into the TAs, while their dc components flowed downstream to be collected at Ω_2 and Ω_4, respectively. The currents I_1 and I_2 were measured to evaluate the dc characteristics of the device by a standard lock-in technique at 31 Hz, while the current noises ΔI_3 and ΔI_5 were measured using the system shown in Fig. 1. We derived the cross correlation $S_{35} = \langle \Delta I_3 \Delta I_5 \rangle$ in the manner explained in Sec. II.

In this setup, $G_{35} = G_{53} = 0$, because the current injected into the sample from Ω_5 (Ω_3) is collected at Ω_4 (Ω_2) and cannot reach Ω_3 (Ω_5). Therefore, we can expect that S_{35} consists of only the shot-noise term $S_{35}{}^{\rm shot}$ as discussed in Sec. II. For the $\nu = 2$ integer QH state, $S_{35}{}^{\rm shot}$ is calculated with the factor $F = [\Sigma_\sigma T_\sigma(1 - T_\sigma)]/2$, where σ denotes the spin direction ($\sigma = \uparrow$ or $\downarrow$).[1] Here T_σ is the transmission probability of the QPC for each edge channel in the lowest Landau level. Since T_σ can be evaluated from the dc transport measurements, the measured S_{35} can be compared with Eq. (1) with only one fitting parameter T_e.

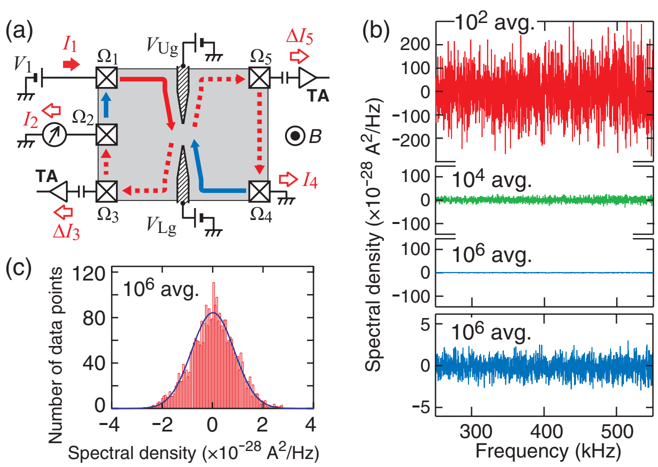

FIG. 5. (a) Schematic of QH device and measurement setup. (b) $S_{35}(f)$ obtained by averaging 10^2 (red), 10^4 (green), and 10^6 (blue) single-shot spectral densities. The lowest graph shows an expanded view of the 10^6 data. (c) Histogram analysis for $S_{35}(f)$ with 10^6 averaging [lowest data in (b)]. Red bars show the number of data points in the measured spectral density and blue solid line is its Gaussian fit.

B. Averaging and histogram analysis

In this subsection, we describe the analysis to find the proper noise floor of the measurement. The noise spectral densities $S_{35}(f)$ were measured at $V_1 = 0$ V in the absence of a QPC by setting $V_{\rm Ug} = V_{\rm Lg} = 0$ V, i.e., no shot noise. Here $V_{\rm Ug}$ and $V_{\rm Lg}$ are the lower and upper gate voltages applied to the QPC gates, respectively. In this case, we expect $S_{35} = 0$ because $S_{35}{}^{\rm shot} = 0$. Figure 5(b) compares the results obtained by averaging 10^2, 10^4, and 10^6 single-shot measurements. The data are scattered around $S_{35}(f) = 0$, consistent with the expectation that $S_{35} = 0$. This confirms that crosstalk between the signal lines is negligible in our measurement setup, because if the crosstalk existed, it would induce finite S_{35}. The fluctuation around $S_{35}(f) = 0$ is because of the extrinsic noise generated in the TAs. The variance of the data rapidly decreases as the averaging count is increased, indicating that lower noise floor is attained with longer time averaging. Note that since it takes time to acquire a large number of spectral densities (typically, it takes about 1 min to obtain 10^4 spectral densities), the averaging count should be chosen according to the purpose of the measurement.

In the following measurements, we derive S_{35} as the mean value of $S_{35}(f)$ in the frequency band from 200 to 500 kHz by performing a histogram analysis, instead of simply averaging $S_{35}(f)$. It allows us to remove the effect of unwanted spike noises, which, although not seen in Fig. 5(b), sometimes appear at certain frequencies. Figure 5(c) shows the histogram of the data in the 200−500 kHz range obtained with 10^6 averaging [the lowest data in Fig. 5(b)]. We fit the histogram with a Gaussian function and determined S_{35} as the center value of the peak. The obtained S_{35} matches zero with a high accuracy within 1×10^{-29} A^2/Hz, demonstrating the validity of our analysis.

C. Shot noise in a quantum point contact

In this subsection, we present shot-noise measurements using the cross-correlation technique described above. The QPC partitions the current I_1 and generates shot noise. Its transmission probability T_σ was tuned with $V_{\rm Lg}$, while fixing $V_{\rm Ug}$ at −0.6 V. Figure 6(a) shows the measured conductance G_{41} from Ω_1 to Ω_4 as a function of $V_{\rm Lg}$. Since the $\nu = 2$ QH state has two co-propagating edge channels (outer up-spin and inner down-spin channels), $G_{41} = 2e^2/h$ at $V_{\rm Lg} = 0$ V. With decreasing $V_{\rm Lg}$, G_{41} decreases showing a well-developed plateau at $G_{41} = e^2/h$ for -0.9 V $< V_{\rm Lg} < -0.5$ V. This indicates that at $V_{\rm Lg} < -0.5$ V, only the outer up-spin channel

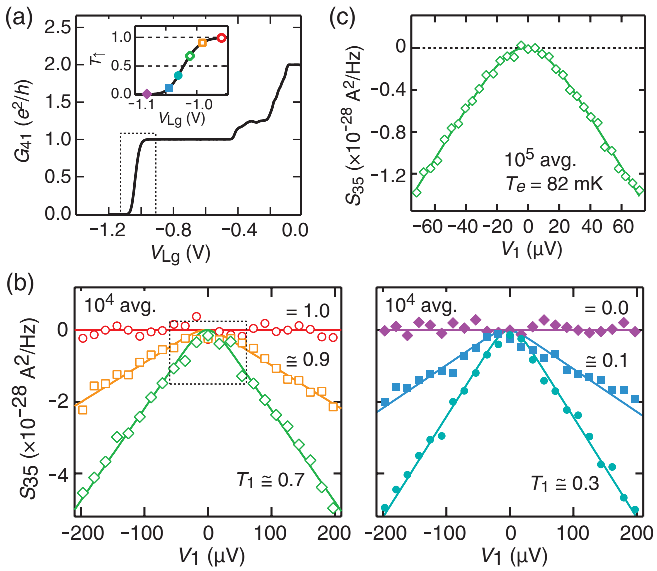

FIG. 6. (a) G_{41} as a function of V_{Lg} while fixing V_{Ug} at -0.6 V. (Inset) $T_\uparrow$ evaluated from measured G_{41} in the dotted area of the main panel. (b) Shot noise as a function of V_1 measured at several $T_\uparrow$ values [marked in the inset of (a)]. Solid lines are theoretical curves calculated with Eq. (1) assuming $T_e = 80$ mK. The data were obtained with averaging of 10^4 spectral densities. (c) Shot noise at $T_\uparrow \cong 0.7$ measured with 10^5 averaging in the bias window indicated by the dotted rectangle in (b). Solid line is the theoretical curve calculated with Eq. (1) assuming $T_e = 82$ mK.

can transmit through the QPC (i.e., $T_\downarrow = 0$). Therefore, in the region below the plateau ($0 \le G_{41} \le e^2/h$) [highlighted by the dotted rectangle in Fig. 6(a)], G_{41} can be converted into $T_\uparrow$ using the relation $G_{41} = (e^2/h)\Sigma_\sigma T_\sigma$.

Figure 6(b) shows S_{35} measured at several V_{Lg} values, marked as points in the inset of Fig. 6(a), plotted as a function of the applied bias voltage V_1. The data were obtained by averaging 10^4 spectral densities. At $T_\uparrow = 0$ or 1 (the opaque red circles or filled purple diamonds, respectively), $S_{35} \cong 0$ independent of V_1. In contrast, at intermediate values of $T_\uparrow$ ($0 < T_\uparrow < 1$), S_{35} decreases from $S_{35} \cong 0$ with increasing $|V_1|$, indicating the generation of shot noise. As discussed in Subsection IV B, we can expect $S_{35} = S_{35}^{\text{shot}}$ to hold in the present setup. Indeed, the S_{35} data show good agreement with the theoretical curves calculated with Eq. (1) assuming $T_e = 80$ mK. This confirms the effectiveness of our cross-correlation technique for shot-noise measurements.

The noise floor of the cross-correlation measurement can be improved by increasing the averaging count. In Fig. 6(c), we show S_{35} at $T_\uparrow \cong 0.7$ obtained by averaging over 10^5 single-shot spectral densities, which can be compared with that for 10^4 averaging in Fig. 6(b). The data demonstrate a dramatic improvement in precision, exhibiting better agreement with the theoretical curve (green solid line). Fitting the data yields $T_e = 82$ mK, indicating that T_e can be evaluated more precisely by increasing the averaging.[17]

V. SUMMARY

We presented a system for cross-correlation measurements using homemade TAs. First, the system exhibits a sufficiently low noise floor for shot-noise measurements when appropriate averaging and histogram analyses are performed. Second, the frequency band of this system is sufficiently high to avoid $1/f$ disturbances in semiconductor mesoscopic devices. Third, the low input impedance of the TAs allows us to reduce crosstalk between two measurement wires to a negligible level. The high performance of the system is confirmed by shot-noise measurements in a QH device and their quantitative analysis. While we focused on shot-noise measurements in this study, the developed system can be utilized for more elaborate cross-correlation measurements aimed at elucidating, for example, the quantum statistics of quasiparticles and/or two-particle interference.[7]

ACKNOWLEDGMENTS

We appreciate the experimental support given by K. Matsuda and M. Ueki. This study was supported by the Grants-in-Aid for Scientific Research (21000004, 21810006, and 25800176).

[1] Ya. M. Blanter and M. Büttiker, Phys. Rep. **336**, 1 (2000).
[2] L. Saminadayar, D. C. Glattli, Y. Jin, and B. Etienne, Phys. Rev. Lett. **79**, 2526 (1997).
[3] R. De-Picciotto, M. Reznikov, M. Heiblum, V. Umansky, G. Bunin, and D. Mahalu, Nature (London) **389**, 162 (1997).
[4] P. Roche, J. Ségala, D. C. Glattli, J. T. Nicholls, M. Pepper, A. C. Graham, K. J. Thomas, M. Y. Simmons, and D. A. Ritchie, Phys. Rev. Lett. **93**, 116602 (2004).
[5] L. DiCarlo, Y. Zhang, D. T. McClure, D. J. Reilly, C. M. Marcus, L. N. Pfeiffer, and K. W. West, Phys. Rev. Lett. **97**, 036810 (2006).
[6] S. Nakamura, M. Hashisaka, Y. Yamauchi, S. Kasai, T. Ono, and K. Kobayashi, Phys. Rev. B **79**, 201308(R) (2009).
[7] P. Samuelsson and M. Büttiker, J. Low Temp. Phys. **146**, 115 (2006).
[8] W. D. Oliver, J. Kim, R. C. Liu, and Y. Yamamoto, Science **284**, 299 (1999).
[9] M. Henny, S. Oberholzer, C. Strunk, T. Heinzel, K. Ensslin, M. Holland, and C. Schönenberger, Science **284**, 296 (1999).
[10] S. Oberholzer, E. Rieri, C. Schönenberger, M. Giovannini, and J. Faist, Phys. Rev. Lett. **96**, 046804 (2006).
[11] A. Das, Y. Ronen, M. Heiblum, D. Mahalu, A. V. Kretinin, and H. Shtrikman, Nature Commun. **3**, 1165 (2012).
[12] L. DiCarlo, Y. Zhang, D. T. McClure, C. M. Marcus, L. N. Pfeiffer, and K. W. West, Rev. Sci. Instrum. **77**, 073906 (2006).
[13] M. Reznikov, M. Heiblum, H. Shrtikman, and D. Mahalu, Phys. Rev. Lett. **75**, 3340 (1995).
[14] A. Kumar, L. Saminadayar, D. C. Glattli, Y. Jin, and B. Etienne, Phys. Rev. Lett. **76**, 2778 (1996).
[15] M. Hashisaka, Y. Yamauchi, S. Nakamura, S. Kasai, T. Ono, and K. Kobayashi, Phys. Rev. B **78**, 241303(R) (2008).
[16] C. Dekker, A. J. Scholten, F. Liefrink, R. Eppenga, H. van Houten, and C. T. Foxon, Phys. Rev. Lett. **66**, 2148 (1991).
[17] L. Spietz, K. W. Lehnert, I. Siddiqi, and R. J. Schoelkoph, Science **300**, 1929 (2003).
[18] M. Hashisaka, Y. Yamauchi, K. Chida, S. Nakamura, K. Kobayashi, and T. Ono, Rev. Sci. Instrum. **80**, 096105 (2009).